Validation of NASA Thermal Ice Protection Computer Codes

Computer Codes

Part 3: The Validation of Antice

Kamel M. Al-Khalil and Charles Horvath
Cox & Company, Inc., New York, New York

Dean R. Miller
Glenn Research Center, Cleveland, Ohio

William B. Wright
NYMA, Inc., Brook Park, Ohio

The NASA STI Program Office . . . in Profile

Since its founding, NASA has been dedicated to the advancement of aeronautics and space science. The NASA Scientific and Technical Information (STI) Program Office plays a key part in helping NASA maintain this important role.

The NASA STI Program Office is operated by Langley Research Center, the Lead Center for NASA's scientific and technical information. The NASA STI Program Office provides access to the NASA STI Database, the largest collection of aeronautical and space science STI in the world. The Program Office is also NASA's institutional mechanism for disseminating the results of its research and development activities. These results are published by NASA in the NASA STI Report Series, which includes the following report types:

- TECHNICAL PUBLICATION. Reports of completed research or a major significant phase of research that present the results of NASA programs and include extensive data or theoretical analysis. Includes compilations of significant scientific and technical data and information deemed to be of continuing reference value. NASA's counterpart of peer-reviewed formal professional papers but has less stringent limitations on manuscript length and extent of graphic presentations.

- TECHNICAL MEMORANDUM. Scientific and technical findings that are preliminary or of specialized interest, e.g., quick release reports, working papers, and bibliographies that contain minimal annotation. Does not contain extensive analysis.

- CONTRACTOR REPORT. Scientific and technical findings by NASA-sponsored contractors and grantees.

- CONFERENCE PUBLICATION. Collected papers from scientific and technical conferences, symposia, seminars, or other meetings sponsored or cosponsored by NASA.

- SPECIAL PUBLICATION. Scientific, technical, or historical information from NASA programs, projects, and missions, often concerned with subjects having substantial public interest.

- TECHNICAL TRANSLATION. English-language translations of foreign scientific and technical material pertinent to NASA's mission.

Specialized services that complement the STI Program Office's diverse offerings include creating custom thesauri, building customized data bases, organizing and publishing research results . . . even providing videos.

For more information about the NASA STI Program Office, see the following:

- Access the NASA STI Program Home Page at *http://www.sti.nasa.gov*

- E-mail your question via the Internet to help@sti.nasa.gov

- Fax your question to the NASA Access Help Desk at 301–621–0134

- Telephone the NASA Access Help Desk at 301–621–0390

- Write to:
  NASA Access Help Desk
  NASA Center for AeroSpace Information
  7121 Standard Drive
  Hanover, MD 21076

Validation of NASA Thermal Ice Protection Computer Codes

Part 3: The Validation of Antice

Kamel M. Al-Khalil and Charles Horvath
Cox & Company, Inc., New York, New York

Dean R. Miller
Glenn Research Center, Cleveland, Ohio

William B. Wright
NYMA, Inc., Brook Park, Ohio

National Aeronautics and
Space Administration

Glenn Research Center

Acknowledgments

This work was sponsored by the Icing Technology Branch at the NASA Glenn Research Center, Cleveland, Ohio.

VALIDATION OF NASA THERMAL ICE PROTECTION COMPUTER CODES
PART 3: THE VALIDATION OF ANTICE

Kamel M. Al-Khalil*, Charles Horvath**
Cox & Company, Inc.
200 Varick Street
New York, New York 10014

Dean R. Miller†
National Aeronautics and Space Administration
Glenn Research Center
21000 Brookpark Road
Cleveland, Ohio 44135

William B. Wright‡
NYMA, Inc.
2001 Aerospace Parkway
Brook Park, Ohio 44142

ABSTRACT

An experimental program was generated by the Icing Technology Branch at NASA Glenn Research Center to validate two ice protection simulation codes: LEWICE/Thermal for transient electrothermal de-icing and anti-icing simulations, and ANTICE for steady state hot gas and electrothermal anti-icing simulations. An electrothermal ice protection system was designed and constructed integral to a 36 inch chord NACA0012 airfoil. The model was fully instrumented with thermocouples, RTD's, and heat flux gages. Tests were conducted at several icing environmental conditions during a two week period at the NASA Glenn Icing Research Tunnel. Experimental results of running-wet and evaporative cases were compared to the ANTICE computer code predictions and are presented in this paper.

Nomenclature

AOA	= angle of attack of body with the freestream air (degrees)
C_{pw}	= specific heat (Btu/lbm.°F)
h	= heat transfer coefficient between the dry surface and the ambient air (Btu/hr.ft^2.°F)
h_f	= film coefficient between the wet surface and the ambient air (Btu/hr.ft^2.°F)
K	= thermal conductivity (Btu/hr.ft.°F)
LWC	= liquid water content in the freestream (g/m^3)
Lv	= water latent heat of vaporization (Btu/lbm)
MVD	= mean volume droplet diameter in cloud (μm)
m	= surface runback mass flow rate per unit span distance (lbm/ft.hr)

m_{evap}	= rate of surface water evaporation (lbm/hr.ft^2)
m_{imp}	= rate of water droplets impingement (lbm/hr.ft^2)
q	= heater power density (W/in^2)
q_{conv}	= convective heat loss (W/in^2)
q_{evap}	= evaporative heat loss (W/in^2)
q_{KE}	= kinetic heat gain from droplets impact on surface (W/in^2)
q_{sens}	= sensible heat required to warm the impinging water droplets (W/in^2)
S	= surface distance from stagnation, positive on the upper surface (in)
T_{aw}	= adiabatic wall temperature (°F)
T_s	= skin temperature (°F)
T_{tot}	= total ambient temperature (°F)
T_∞	= static ambient temperature (°F)
V	= freestream velocity (mph)
β	= droplets collection efficiency
ρ	= mass density (lbm/ft^3)

*Engineering Scientist, Member AIAA
**De-icing Systems Engineer
†Aerospace Engineer, Member AIAA
‡Aerospace Engineer, Member AIAA

I. Introduction

Extensive testing is normally required in the design of thermal ice protection systems. The cost involved can be somewhat prohibitive. Some designers reduce costs by relying upon computer simulations to get through the preliminary design stage. The total cost and development period involved can further be reduced if the simulation codes are proven and reliable. Additionally, the simulation codes may be utilized in the certification process, in conjunction with flight/tunnel testing, once approved by the FAA.

An experimental program was initiated and sponsored by the Icing Technology Branch at the NASA Glenn Research Center (GRC) in an effort to validate two thermal ice protection simulation codes: LEWICE/Thermal simulates the transient response of electrothermal de-icing and anti-icing systems, and ANTICE simulates the steady state response of hot gas and electrothermal anti-icing systems. The effort was a partnership between NASA GRC and five US industry members. Participants from industry assumed the role of technical advisors. Additionally, Cox & Company, Inc. provided the test article, test monitoring and control software/hardware, and engineering test support.

An overview of the program is discussed by Miller,[1] and the validation of the LEWICE/Thermal code is presented by Wright.[2] This particular paper is dedicated to the validation of the ANTICE code which is a two dimensional computer simulation of a composite structure with embedded heaters. It also simulates a hot gas anti-icing system. The code has a rivulet model to simulate the flow of runback water on the surface. Experimental anti-icing data will be presented, and comparison will be made to the ANTICE code predictions.

II. Analytical Model

The computer code is based on an analytical thermodynamic model that was described in earlier studies by Al-Khalil.[3,4] The various modes of heat transfer occurring within an anti-iced aircraft surface and the collected water, referred to as "runback" when it flows on the surface, have been modeled. The mathematical formulation is based on 2-D steady-state heat transfer model along a surface streamline.

The temperature is assumed to vary in the streamwise direction and across the structure thickness (transverse direction). Spanwise variations are much smaller than those in the chordwise direction. The runback water flow is also assumed, as proven in several tunnel tests, to be in the streamwise direction on the aircraft surface.

The aircraft structure may be represented by a number of composite layers. Any single layer can be composed of several heater zones, each with a specified power density. The mathematical formulation of the energy balance equation in the structure is based on the control volume approach. The structure is subdivided into a number of grids in the streamwise and transverse directions. An equation is then written for each node in the discretized region using the laws of energy conservation (and mass conservation on the impinging supercooled water droplets).

Anti-icing of the aircraft surface may also be accomplished using a hot air system. This is currently modeled such that hot air of a given mass flowrate and an initial temperature is supplied to the inner surface in the vicinity of the stagnation line, and flows back into the cowl in the direction of surface streamlines. A user can also specify a distribution of variable heat flux at the surface to obtain an approximate system behavior as a first step in the design and/or analysis process (i.e., evaporative, running wet, or freezing runback).

Also modeled is the runback flow behavior on the surface: continuous surface coverage at the direct impingement regions, versus rivulet structure flow downstream. Rivulets are individual narrow streams of water. A stability analysis was performed for the prediction of rivulets.[3,4]

ANTICE requires the following information:

(1) Surface pressure coefficient distribution along a streamline.
(2) The distance between two adjacent surface streamlines representing a zone of interest in the analysis. This is an option for 3-D flows such as on swept wings or inlet nacelles.
(3) Collection efficiency distribution at the surface.

The above information may be obtained from flow and trajectory codes such as NASA's LEWICE ice accretion code. In the current analytical predictions, LEWICE[5] v1.7 was used to obtain the latter information. Details on the numerical procedure are presented in Reference [4].

III. Experimental setup

III.1   Test Article

A NACA0012 airfoil, 6 ft span and 36" chord, was fitted with an electro-thermal ice protection system at the leading edge (LE) and mounted vertically in the NASA GRC Icing Research Tunnel (IRT). The removable LE was 10" long, and the wooden afterbody was 26" long. The ice protection system consisted of seven heater bands, each 18 inches long in the spanwise direction, individually controlled by the Cox Thermal Test Management System (TTMS). For redundancy, a spanwise image mirror of the seven heaters was constructed around the center line of the airfoil. The total heated spanwise length was 3 ft, and the total heated wrap distance in the chordwise direction was 7.75 inches.

A guard heater (8" span x 12" wrap) was installed on each end of the heated area along the airfoil span. The guard heaters were used to maintain as much of the airfoil clean of ice to prevent flow disturbances from affecting the measurement locations near the centerline. The total number of heated channels was 18.

Figure 1 shows a cross-section of the LE where zone A is 0.75" wide, zones B, C, D, and E are 1" wide, and finally zone F and G are 1.5" wide. Zones B, D, and F are on the IRT control room side. During the manufacturing process, the heater lay-up was accidentally shifted towards zones C, D, and G. The shift was estimated at about 0.19" during the tunnel tests when different amounts of surface runback were observed on each side of the airfoil. This heater shift was modeled in the computer code for a proper comparison between the experimental data and the analytical predictions.

Figure 2 illustrates the material composition of the LE structure in the heated zones, and the estimated/known material properties are given in Table I. This particular type of construction was required to meet the goals set forth for the validation program.

III.2   Test Instrumentation

The model was heavily instrumented with type-T thermocouples, heat flux gages, and Resistance Temperature Detectors (RTD). A total of 76 sensors was used. The locations of several of the sensors are illustrated in Reference [1].

The development of the Cox TTMS began in the early 1980's, and has been used to support the design of ice protection systems for the F-14, OV-1, AH-64, B-1B, and SAAB 340 aircraft, among others. It performs two main functions: data acquisition and closed-loop control. It consists of data acquisition boards to measure analog input signals which are sent to a personal computer via data bus. These signals are converted to digital representation of physical measurements (temperature, heat flux, resistance) with a custom written software. The software then sends signals back to the power module in the TTMS to control the amount of power supplied to individual heater zones.

A user can request the TTMS to maintain a particular sensor at a desired temperature (e.g., to maintain the thermocouple temperature feedback on the metal skin constant). The TTMS will then control in a closed-loop and resolve the power density required for each heater to yield the desired temperature. Conversely, the user can simply set the power density to each heater independent of sensors temperature feedback (TTMS will disconnect the power in case the temperature exceeds a preset value).

Additional equipment was used to monitor the test. Video recorders were used throughout the tests to monitor surface runback and the ice growth. Still photographs were taken with 35 mm cameras to document ice shapes and residual ice following each run. An infrared camera setup was utilized to monitor the airfoil LE surface temperature from the IRT control room. A portion of the LE was coated with a thin black paint to increase the surface emissivity to near 0.96 (Bare metal normally has very low surface emissivity).

III.3   Test Conditions

Anti-icing and de-icing runs were performed at two different airspeeds, several airfoil AOA's, and various meteorological conditions. These icing conditions are summarized in Table II. This paper is dedicated to the validation of the ANTICE program. Therefore, only anti-icing test runs will be discussed (evaporative and running-wet). For simplicity, and to focus on the physical analysis of the icing process with fewer experimental error uncertainties, only cases with zero degrees angle of attack will be considered in the comparison process. The large experimental database generated will be utilized to continue the validation process further.

IV. Energy Balance Analysis and Discussions

Simulation of the icing process of aircraft surfaces is a challenging task. Several uncertainties exist as a result of the large number of variables involved in this problem. In order to understand the differences between the experimental data and the theoretical predictions, the energy balance terms will be illustrated. The various modes of heat transfer will be illustrated to study the contribution of each on the total power required for a running-wet system and an evaporative system.

The energy required to heat the aircraft skin to a specified temperature may be expressed in general terms as:

$$q = q_{conv} + q_{evap} + q_{sens} + q_{KE} \quad (1)$$

where the individual components are written as,

$$q_{conv} = h\,(T_s - T_{aw}) \quad (2)$$

$$q_{evap} = m_{evap}\,L_v \quad (3)$$

$$q_{sens} = m_{imp}\,C_{pw}\,(T_s - T_\infty) \quad (4)$$

$$q_{KE} = m_{imp}\,V^2/(2\,g_c) \quad (5)$$

The runback heat of enthalpy was neglected in Eq. (1) for simplicity in illustrating the point. Besides, this term is negligible when the surface is controlled to a specified temperature in which case the runback is maintained at a constant temperature. The rate of water impingement is:

$$m_{imp} = \beta\,LWC\,V \quad (6)$$

The rate of water evaporation from the surface is a non-linear function of the surface temperature as described in Reference [6].

In order to identify the contribution of each term, two example cases will be considered: a cold condition at -22 °F, and a warm condition at 20 °F. These examples will be useful in the analysis of the ANTICE predictions when compared to the experimental data in the following section. The following parameters were selected as representative values:

h = 40 Btu/hr.ft^2.°F
LWC = 0.39 g/m^3
β = 0.5
V = 200 mph

The heat required to keep the surface at specific range of temperatures was computed using Eq. (1). The total power density as well as each heat component were plotted in Figures 3 and 4 for the warm and cold conditions, respectively. The corresponding results expressed in terms of percentage of the total heat required are illustrated in Figures 5 and 6.

These plots show the strong dependence of total power required for evaporative anti-icing (normally in the range of 100 to 120 °F) on the evaporation rate which is directly related to droplet impingement rates. On the other hand, to maintain the surface just above freezing, for example at 40 °F, the total power required is highly dependent on the convective heat transfer coefficient and ambient temperature.

V. Test Results and Comparisons

Several runs at different icing conditions (see Table I) were executed. Experimental results of most of the runs were summarized in Table III where the Run numbers and the corresponding TTMS file record number are shown. The measured skin temperatures and the heater power densities for each zone are displayed. The results and comparisons to the ANTICE predictions will be illustrated and discussed for each mode of anti-icing separately, running-wet and evaporative.

V.1 Running-wet Anti-icing Cases:

In the running-wet conditions, the runback was maintained at temperatures a few degrees above freezing within the heated region. Beyond this region, the runback freezes along a distance that depends on several variables but mostly on temperature. Figures 10 and 11 show that effect. ANTICE normally predicts freezing within about 0.75" length for cold conditions and about 2" for warm and very wet (high LWC) conditions.

In the validation process, the measured power densities were then used as inputs to the ANTICE code. Comparisons between the predicted and measured skin temperatures will be the basis of validation in this paper. Few example cases will be illustrated as representative to the level of agreement between the theoretical and the experimental data. It is planned that all test runs will be summarized and made available on digital media, such as on a CD-ROM, along with ANTICE predictions for several runs.

In running-wet operations, the surface runback mass flow rate rapidly increases as it moves away from the stagnation line within the direct impingement region. Since a small percentage is evaporating, the runback flow rate should reach a maximum just upstream of the impingement limits, and start to decrease slowly as it flows to downstream regions. To illustrate this phenomenon, consider the case of Run#22B (TTMS#71 as shown in Table III). This corresponds to icing condition 1 as illustrated in Table II.

Figure 12 illustrates the experimental as well as the ANTICE predicted skin temperature and surface mass flow rate distributions. The above discussion of surface mass flow rate is predicted by ANTICE. The surface temperatures are in excellent agreement with the measured values. This was not the case for the aft 2 heaters (D, E, F, and G) when the measured laminar heat transfer coefficients shown in Figures 8 and 9 were used. When the experimental film coefficient for the wet condition was plotted as shown in Figure 13, it was realized that the laminar flow is disturbed by the surface runback water (beads and rivulets) and transition to turbulent flow must have occurred just past about 1.25 inches. Therefore, the flow was manually tripped at those locations, and 2 new heat transfer coefficient distributions (one at 100mph and another at 200mph freestream velocities) were used thereafter in the remainder of the cases.

Additional running-wet cases illustrated in Figures 14 through 17 show a very good agreement with the experimental values. It should be realized that more studies must be conducted to predict the transition locations for different geometries at different airspeeds and surface runback physical structure and dimensions.

V.2 Evaporative Anti-icing Cases:

Evaporative anti-icing predictions were not as good as the running-wet cases. As discussed in Section IV, and as shown in Figures 5 and 6 for temperatures in excess of 100 °F, approximately 70% of the total power required to achieve a fully evaporative operation (no runback beyond the heated zones) is the heat component required to evaporate surface water as given by Equation (3). This is a result of the high latent heat of vaporization of water.

This phenomenon is better understood through an example. Consider Run#22A (TTMS#70). Figure 18 illustrates the experiment film coefficient in a wet environment. The average wet film coefficient should superimpose the dry film or heat transfer coefficient beyond the direct impingement zone where the surface is dry. This occur near +/-2 inches from the hilite. Beyond those locations, the experimental film coefficient increases indicating that transition to turbulence has occurred. In a similar manner to the running-wet conditions, the boundary layer was manually tripped at those locations to predict the heat transfer coefficient distribution which was used for the remainder of the cases at the same freestream velocity.

Figure 19 shows the ANTICE code predictions for the skin temperature and the runback mass flow rate. The comparison is acceptable considering the large surface temperature variations within short distances as also observed in the IR camera thermographic data. Surface runback water disappear near and past the impingement limits confirming an evaporative system operation.

Figure 20 illustrates a typical behavior seen in many of the cases. In low airspeeds, 100mph here, a higher surface temperature is required to achieve full evaporation. The two main elements that promote evaporation are a higher mass transfer coefficient which is proportional to the heat transfer coefficient, and a high surface temperature. This was confirmed in all the experimental results and shown here in two examples: Figure 20 for the low airspeed of 100mph and Figure 21 for the high airspeed 200mph. Both cases were at the same ambient temperature (0 °F). At 100mph, it was noticed that a surface temperature of about 150 °F was required as opposed to 100 °F in the case of 200mph.

Comparisons of the predicted temperatures to the experimental measurements in those two figures is subjective. In many cases, the code seems to predict the stagnation within about 10 °F which is acceptable considering the measurement uncertainties and the number of environmental variables involved. However, the skin temperature at zones B&C, adjacent to the hilite heater, are always underpredicted by ANTICE (by 25 °F or more). This may be associated with two reasons: (1) many of the conditions were near the edge of

the spray bar calibration envelope which could result in smaller LWC than actually predicted by the calibration standard; (2) the predicted rate of mass evaporation is always assumed to get 100% of the latent energy from the skin and absolutely none from the heated boundary layer. A closer look should be given to all variables throughout the icing simulation (experimental and computational).

VI. Concluding Remarks

An experimental program was generated by the Icing Technology Branch at NASA Glenn Research Center to validate two ice protection simulation codes: LEWICE/Thermal and ANTICE. This paper was dedicated to the validation of ANTICE, a steady state hot gas and electrothermal anti-icing simulations. An electrothermal ice protection system was designed and constructed integral to a 36 inch chord NACA0012 airfoil. The model was fully instrumented with thermocouples, RTD's, and heat flux gages. Tests were successfully conducted at several icing environmental conditions in the NASA Glenn Icing Research Tunnel (IRT). Experimental results of running-wet and evaporative cases were compared to the ANTICE computer code predictions.

The dry heat transfer coefficients predicted by LEWICE, when forced to stay laminar, were in general good agreement with the measured values. This distribution was slightly higher in the experimental cases than in the theoretical predictions. The difference can be attributed to the fact that the IRT is not considered as a low turbulence aerodynamic tunnel and its main purpose is to simulate icing environments. In the validation process, the experimental values were used in the laminar region to isolate the effect of that variable on the ANTICE temperature predictions.

The computer code predictions for running-wet anti-icing conditions were very close to the experimental measurements. However, this agreement near the aft zone heaters was realized when the laminar boundary layer (BL) was forced to trip at these locations as depicted in the experimental results of the film coefficient distribution in wet conditions.

The ANTICE code predictions of the skin temperatures in the evaporative cases were acceptable near stagnation, but marginal elsewhere especially at zones B&C. This is due to the large effects of the evaporative cooling which is directly attributed to the high latent heat of vaporization of water. An accurate measurement of LWC and verification of the collection efficiency distribution are required to evaluate any deficiencies in the standard evaporative terms used in most icing simulation codes. Nevertheless, ANTICE predicted no runback existed past the heated zones in most cases. Interestingly, evaporative anti-icing is more dependent on the power requirements and not the standard surface temperature of 120 °F normally assumed. In low velocity conditions (low h), the surface reached over 150 °F to achieve fully evaporative conditions.

One should not expect to always correctly predict the skin temperature at the aft heater zones because the difference between having little or no runback at those regions can be as high as 100 °F. Heaters at those regions must be designed such that they protect against the majority of icing condition requirements without exceeding the material temperature limits in the dry conditions at the low aircraft airspeed of its operational envelope.

Future recommended studies:

1. Develop a model that will predict the transition location and the heat transfer coefficients for different conditions. The BL seems laminar for a relatively wide portion of the leading edge (LE) as opposed to what LEWICE normally predicts. Experimental results show that the BL is definitely affected by surface water runback (beads and rivulets). The transition location is moved further downstream in evaporative anti-icing cases but the transition to turbulent is milder.

2. Revisit the evaporative cooling law as applied to aircraft icing. Studies of the basic physics must be conducted to isolate the various modes of heat transfer, especially the evaporative mass and energy transfer from the surface. These studies must also verify the cloud LWC and the water droplet collection efficiency at the LE of the model. The effect of heating the surface and evaporation on the BL must also be considered.

3. Carefully analyze all the records in the relatively large experimental database, and conduct a thorough validation process with sensitivity analysis. This, for example, includes verification of thermocouple readings with thermographic data from the Infrared camera.

References

[1]Miller, D.R., Bond, T.H., Sheldon, D.W., Wright, W.B., Langhals, T., Al-Khalil, K.M., Broughton, H., "Validation of NASA Thermal Ice Protection Computer Codes: Part 1 - Program Overview", AIAA Paper 97-0049, Jan 1997.

[2]Wright, W.B., Al-Khalil, K.M., Miller, D.R., "Validation of NASA Thermal Ice Protection Computer Codes: Part 2 - The Validation of LEWICE/Thermal", AIAA Paper 97-0050, Jan 1997.

[3]Al-Khalil, K.M., Keith, T.G., and De Witt, K.J., "Further Development of an Anti-Icing Runback Model," AIAA Paper 91-0266, Jan. 1991.

[4]Al-Khalil, K.M., Keith, T.G., and De Witt, K.J., "Development of an Improved Model for Runback Water on Aircraft Surfaces," AIAA Paper 92-0042, Jan. 1992.

[5]Wright, W.B., "Users Manual for the Improved NASA Lewis Ice Accretion Code LEWICE 1.6", NASA CR-198355, June 1995.

[6]Al-Khalil, K.M., Keith, T.G., De Witt, K.J., Nathman, J.K., Dietrich, D.A., "Thermal Analysis of Engine Inlet Anti-Icing Systems," *Journal of Propulsion and Power*, Vol. 6, No. 5, Sept-Oct, 1990, pp. 628-634.

Table I: Leading Edge Material Properties

ITEM	MATERIAL	K (Btu/hr.ft.°F)	ρ (lbm/ft^3)	C_p (Btu/lbm.°F)
1	Heating Element (alloy 90)	23.7	556	0.092
2	Erosion Shield (SS 301 HH)	9.4	501	0.12
3	Elastomer (Cox 4300)	0.148	86.4	0.30 +/-0.03
4	Fiberglass/Epoxy Composite	0.17	112	0.375
5	Silicone Foam Insulation	0.07	40.5	0.27 +/-0.03

Table II: Icing Conditions Tested at the NASA GRC IRT

Icing Condition	T_{tot} (°F)	V (mph)	LWC (g/m^3)	MVD (µm)	AOA (degrees)
1	20	100	.78	20	0
2	20	100	1.1	20	0
3	20	200	.39	20	0
4	0	100	.78	20	0
5	0	100	1.1	20	0
6	0	200	.39	20	0
7	20	200	.55	20	0
8	0	200	.55	20	0
9	20	100	.78	20	-2
10	20	100	.78	20	-4
11	20	100	.90	40	0
12	-22	200	.39	20	0
13	15	100	2.0	20	0
14	0	100	.78	20	-2
15	0	100	.78	20	-4

Table III: Summary of Measured Skin Temperatures and Heater Power Densities
(Evaporative and Running-wet Anti-Icing Modes)

| Icing Cond-ition	Run # (TTMS#)	Anti-Icing Mode	Zone A		Zone B		Zone C		Zone D		Zone E		Zone F		Zone G	
			T_s	q	T_s	q	T_s	q	T_s	q	T_s	q	T_s	q	T_s	q
1	22 (70,71)	Evap	117	30	147	21	150	12	160	6.6	162	4.5	157	6.4	156	6.6
		Wet	38	3.1	40	2.6	40	1.9	40	1.9	39	2.2	40	1.7	38	1.5
2	48 (75,76)	Evap	116	30	158	27	163	19	169	8.2	172	4.3	165	7.6	164	8.8
		Wet	37	3.2	39	2.6	40	2.3	39	2.0	39	2.3	38	1.7	39	1.7
3	53 (80,81)	Evap	92	24	97	17	100	12	103	6.7	106	3.0	100	6.2	101	5.3
		Wet	36	4.2	38	3.4	38	3.4	37	3.5	36	3.8	35	2.6	35	2.4
4	35 (63,64)	Evap	112	30	144	22	151	15	154	7.6	157	4.3	150	7.8	149	8.2
		Wet	36	5.8	38	4.5	39	3.8	38	3.8	38	4.0	36	3.1	36	2.9
5	58 (114,115)	Evap	112	30	133	25	155	22	163	11	174	8.0	153	11	159	12
		Wet	38	6.3	41	4.8	40	3.6	42	4.2	40	4.2	41	3.4	40	3.2
6	63 (116,117)	Evap	92	27	98	19	102	14	102	9.3	105	5.4	93	11	89	9.4
		Wet	47	10	48	8.0	49	7.2	47	9.1	47	9.1	46	6.7	46	6.3
7	65 (101,102)	Evap	102	30	128	28	135	22	145	10	151	3.1	142	5.6	136	9.3
		Wet	38	4.9	39	3.8	39	3.6	38	4.0	38	4.4	37	3.1	37	2.9
8	67 (104,105)	Evap	91	28	97	21	99	17	100	14	101	12	94	13	95	12
		Wet	42	9.8	43	7.0	45	6.4	43	7.7	42	8.3	38	5.4	42	5.6
9	69 (92,93)	Evap	117	30	164	18	163	19	170	6.1	172	3.8	164	8.7	169	4.9
		Wet	38	3.1	40	2.6	40	1.9	40	1.9	40	1.9	39	1.7	39	1.7
10	71 (95,96)	Evap	117	30	154	13	151	24	154	6.6	160	5.4	147	11	135	4.5
		Wet	39	3.5	41	2.6	39	1.9	41	2.5	40	2.0	40	2.0	40	2.0
11	73 (98,99)	Evap	116	30	141	27	150	22	157	9.2	168	5.3	157	7.7	154	8.4
		Wet	40	4.0	41	2.8	42	2.6	42	2.5	40	2.5	41	2.0	41	2.0
12	75 (124,125)	Evap	91	30	122	28	125	23	132	11	132	11	116	15	102	15
		Wet	45	15	47	10	47	9.0	46	12	45	13	44	9.4	45	8.9
13	87 (110)	Evap	--	--	--	--	--	--	--	--	--	--	--	--	--	--
		Wet	37	4.6	39	3.5	39	2.6	39	2.5	39	2.5	39	2.2	38	2.0
14	89 (119)	Evap	114	30	175	22	168	24	190	8.9	192	5.0	167	12	168	6.4
		Wet	--	--	--	--	--	--	--	--	--	--	--	--	--	--
15	91 (122,123)	Evap	113	30	160	16	151	28	161	11	166	5.5	153	14	160	7.8
		Wet	40	6.3	43	4.5	42	3.9	43	4.7	43	3.4	43	3.9	43	3.7
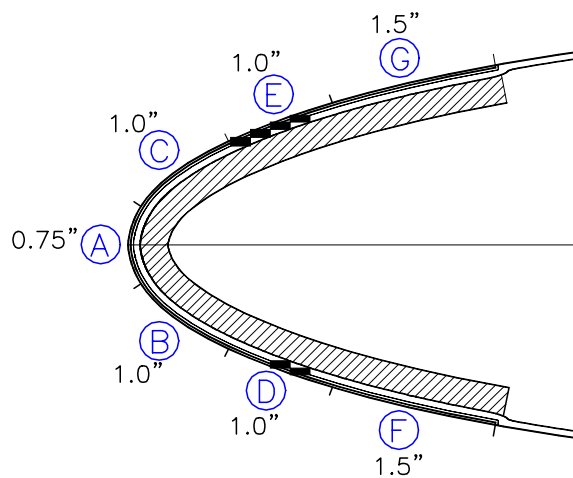
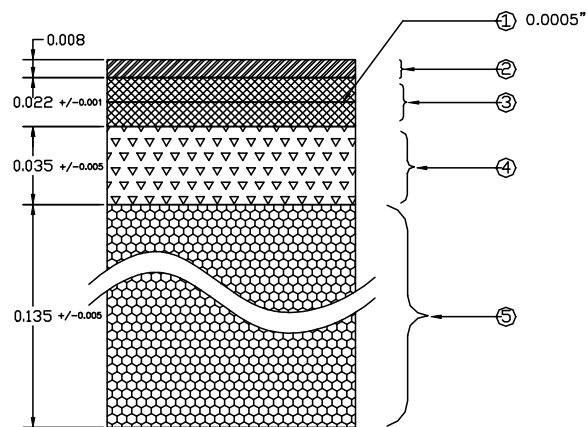Figure 1: Cross-section of the airfoil leading edge and heated zones

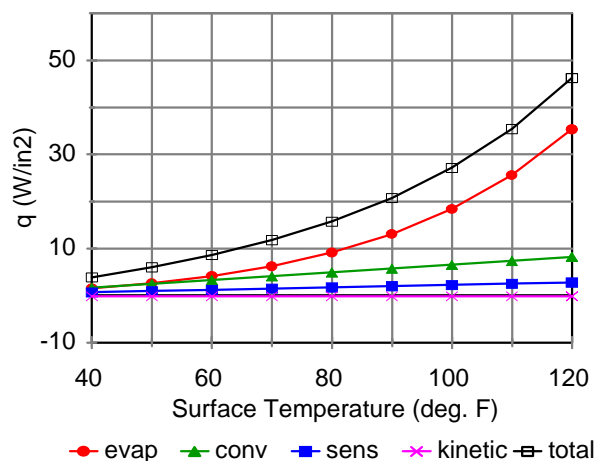

Figure 2: Leading edge material composition (see Table I)

Figure 3: Energy balance terms at $T_{tot} = 20\ ^oF$

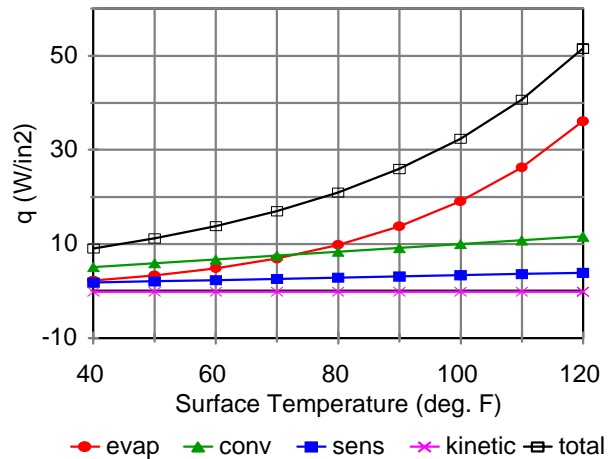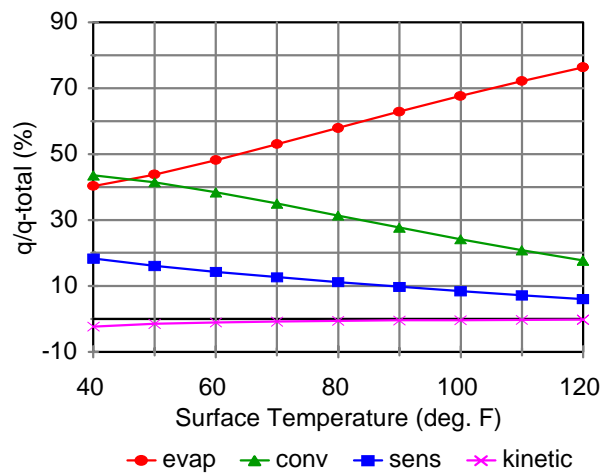Figure 4: Energy balance terms at $T_{tot} = -22\ ^oF$

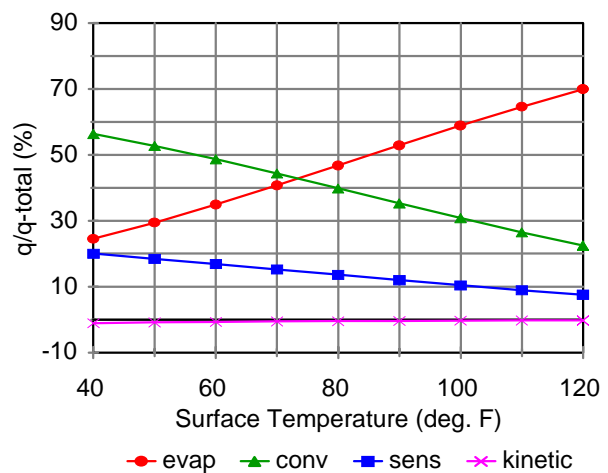Figure 5: Energy balance terms at $T_{tot} = 20\ ^oF$ in percentage of total heat required

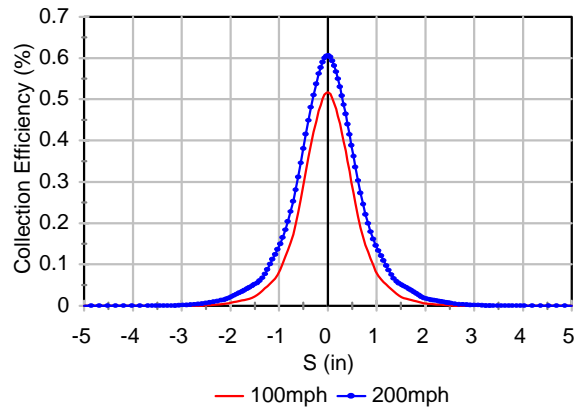Figure 6: Energy balance terms at $T_{tot} = -22\ ^oF$ in percentage of total heat required
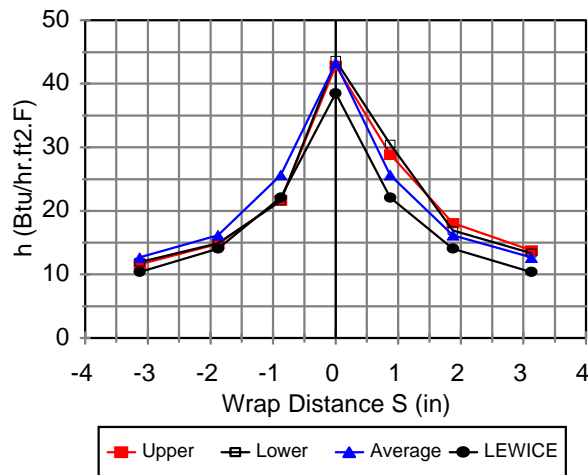
Figure 7:   Predicted collection efficiencies

Figure 10: Typical runback in a running-wet anti-
icing case at cold ambient temperatures

Figure 8:   Experimental and LEWICE predictions
of h at V=100mph (Run#22, TTMS#51)
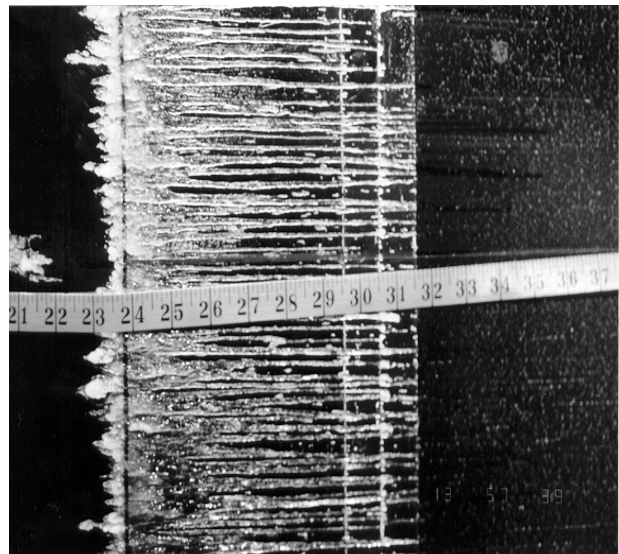
Figure 11: Typical runback in a running-wet anti-
icing case at warm ambient
temperatures

Figure 9:   Experimental and LEWICE predictions
of h at V=200mph (Run#13, TTMS#42)
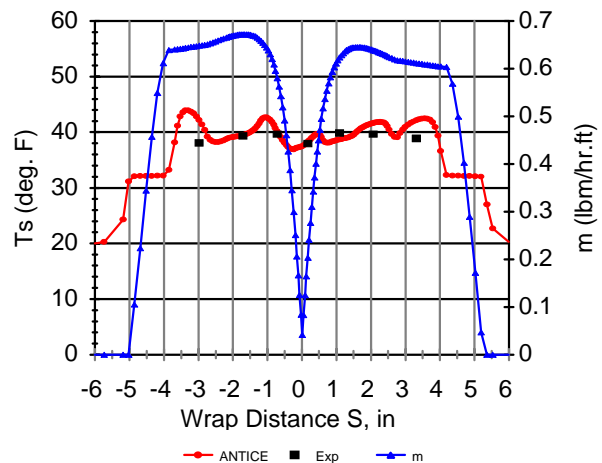
Figure 12: Experimental and ANTICE predictions
for Run#22B (TTMS#71, running-wet)
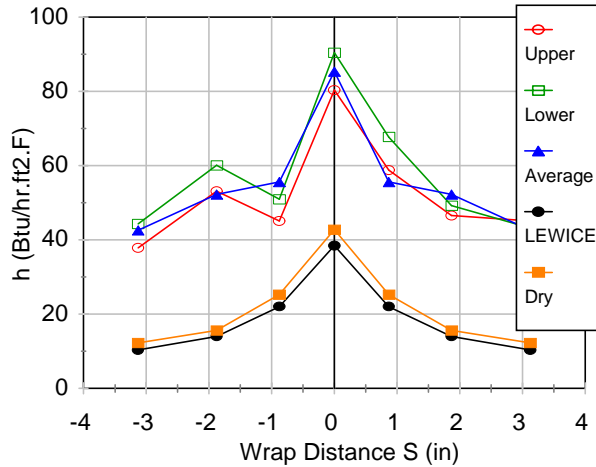
Figure 13: Experimental film coefficient for Run#22B (TTMS#71, running-wet)
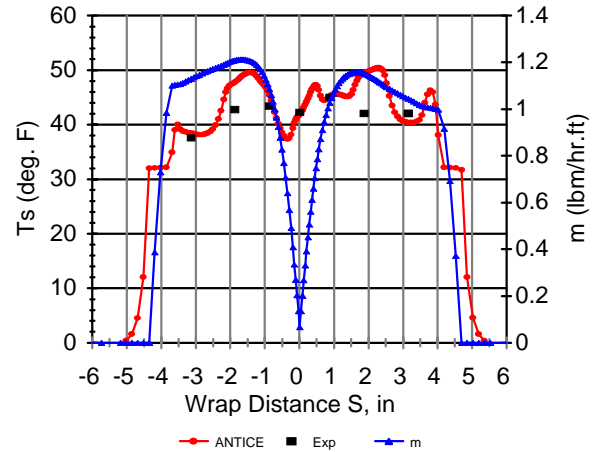
Figure 16: Experimental and ANTICE predictions for Run#67B (TTMS#105, running-wet)
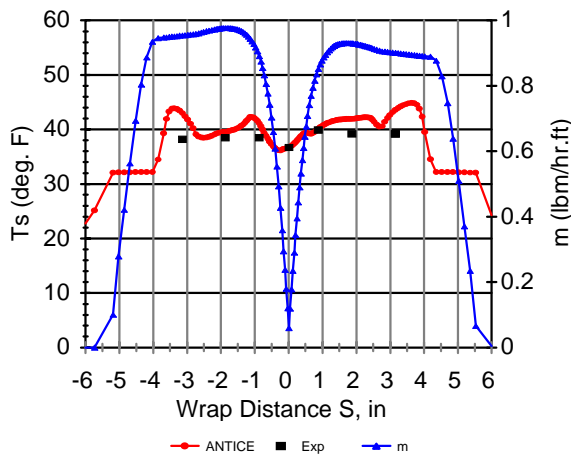
Figure 14: Experimental and ANTICE predictions for Run#48B (TTMS#76, running-wet)
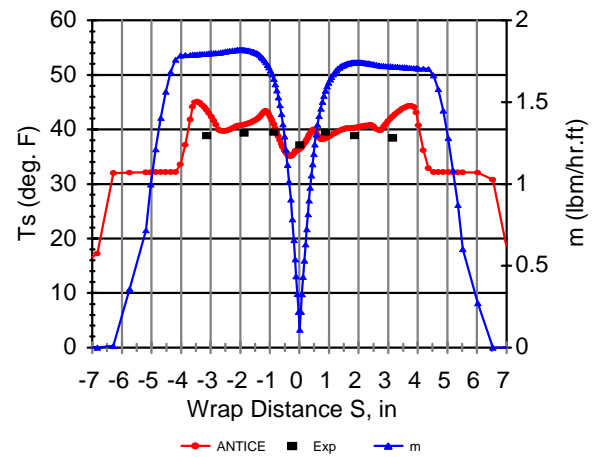

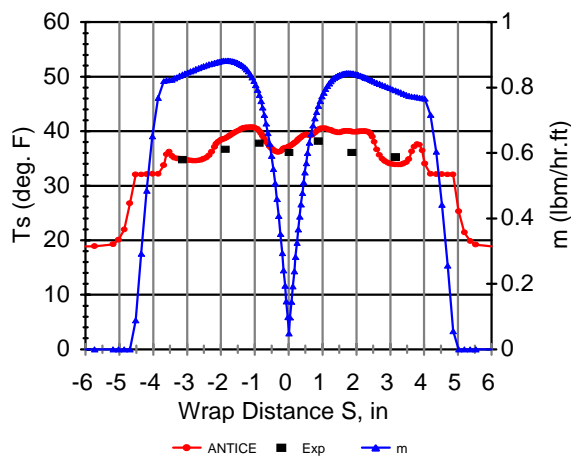*Figure 17: Experimental and ANTICE predictions for Run#87 (TTMS#110, running-wet)*

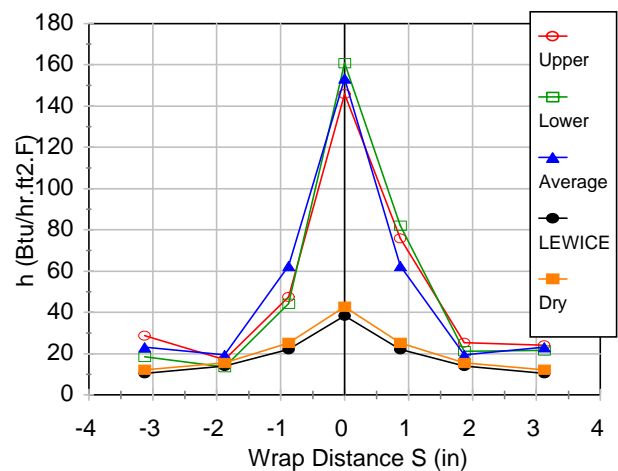*Figure 15: Experimental and ANTICE predictions for Run#53B (TTMS#81, running-wet)*

Figure 18: Experimental film coefficient for Run#22A (TTMS#70, evaporative)
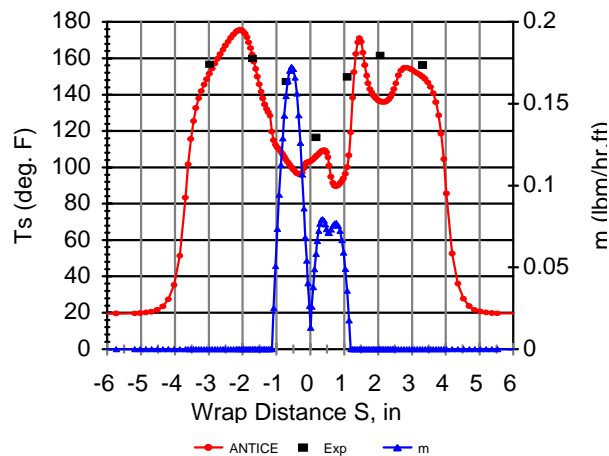
Figure 19: Experimental and ANTICE predictions for Run#22A (TTMS#70, evaporative)
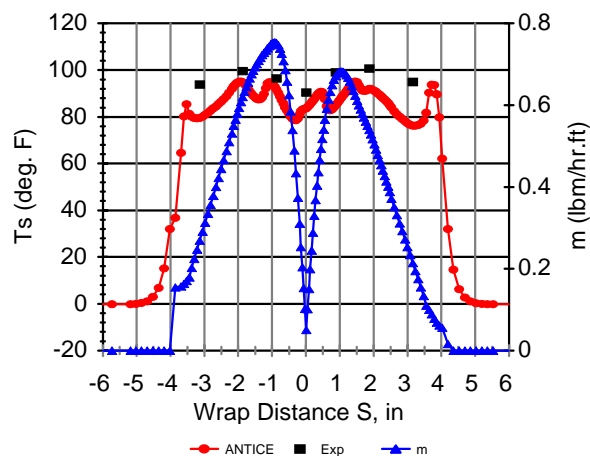

Figure 21: Experimental and ANTICE predictions for Run#67A (TTMS#104, evaporative)
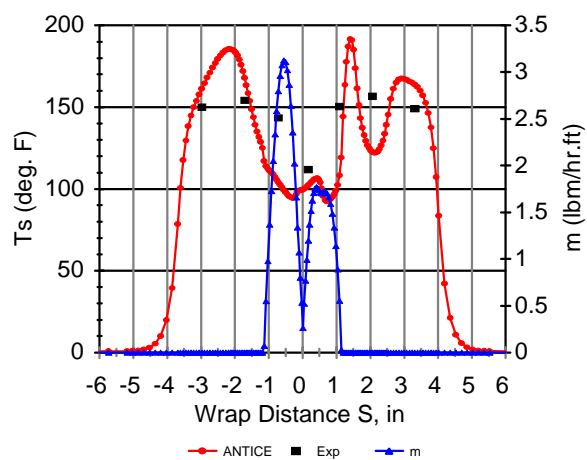

Figure 20: Experimental and ANTICE predictions for Run#35A (TTMS#63, evaporative)

REPORT DOCUMENTATION PAGE

Public reporting burden for this collection of information is estimated to average 1 hour per response, including the time for reviewing instructions, searching existing data sources, gathering and maintaining the data needed, and completing and reviewing the collection of information. Send comments regarding this burden estimate or any other aspect of this collection of information, including suggestions for reducing this burden, to Washington Headquarters Services, Directorate for Information Operations and Reports, 1215 Jefferson Davis Highway, Suite 1204, Arlington, VA 22202-4302, and to the Office of Management and Budget, Paperwork Reduction Project (0704-0188), Washington, DC 20503.

1. AGENCY USE ONLY (Leave blank)	2. REPORT DATE	3. REPORT TYPE AND DATES COVERED
	May 2001	Technical Memorandum

4. TITLE AND SUBTITLE

Validation of NASA Thermal ice Protection Computer Codes

Part 3: The Validation of Antice

6. AUTHOR(S)

Kamel M. Al-Khalil, Charles Horvath, Dean R. Miller, and William B. Wright

5. FUNDING NUMBERS

WU–711–21–23–00

7. PERFORMING ORGANIZATION NAME(S) AND ADDRESS(ES)

National Aeronautics and Space Administration
John H. Glenn Research Center at Lewis Field
Cleveland, Ohio 44135–3191

8. PERFORMING ORGANIZATION REPORT NUMBER

E–12786

9. SPONSORING/MONITORING AGENCY NAME(S) AND ADDRESS(ES)

National Aeronautics and Space Administration
Washington, DC 20546–0001

10. SPONSORING/MONITORING AGENCY REPORT NUMBER

NASA TM—2001-210907
AIAA–97–0051

11. SUPPLEMENTARY NOTES

Prepared for the 35th Aerospace Sciences Meeting and Exhibit sponsored by the American Institute of Aeronautics and Astronautics, Reno, Nevada, January 6–7, 1997. Kamel M. Al-Khalil and Charles Horvath, Cox & Company, Inc., 200 Varick Street, New York, New York 10014; Dean R. Miller, NASA Glenn Research Center; and William B. Wright, NYMA, Inc., 2001 Aerospace Parkway, Brook Park, Ohio 44142. Responsible person, Dean R. Miller, organization code 5840, 216–433–5349.

12a. DISTRIBUTION/AVAILABILITY STATEMENT

Unclassified - Unlimited
Subject Category: 03   Distribution: Nonstandard

Available electronically at http://gltrs.grc.nasa.gov/GLTRS

This publication is available from the NASA Center for AeroSpace Information, 301–621–0390.

12b. DISTRIBUTION CODE

13. ABSTRACT (Maximum 200 words)

An experimental program was generated by the Icing Technology Branch at NASA Glenn Research Center to validate two ice protection simulation codes: LEWICE/Thermal for transient electrothermal de-icing and anti-icing simulations, and ANTICE for steady state hot gas and electrothermal anti-icing simulations. An electrothermal ice protection system was designed and constructed integral to a 36 inch chord NACA0012 airfoil. The model was fully instrumented with thermocouples, RTD's, and heat flux gages. Tests were conducted at several icing environmental conditions during a two week period at the NASA Glenn Icing Research Tunnel. Experimental results of running-wet and evaporative cases were compared to the ANTICE computer code predictions and are presented in this paper.

14. SUBJECT TERMS

Aircraft ice protection; Thermal ice protection

15. NUMBER OF PAGES

18

16. PRICE CODE

17. SECURITY CLASSIFICATION OF REPORT	18. SECURITY CLASSIFICATION OF THIS PAGE	19. SECURITY CLASSIFICATION OF ABSTRACT	20. LIMITATION OF ABSTRACT
Unclassified	Unclassified	Unclassified	